Dyes and Pigments 229 (2024) 112280

Contents lists available at ScienceDirect

Dyes and Pigments

journal homepage: www.elsevier.com/locate/dyepig

The impressive colors of the *bis*-aminostyrylbenzopyrylium system. Evidence by stopped-flow for the B4 formation at pH>13

Paula Araújo [a], Alexandra Borges [a], Joana Oliveira [a,*], André Seco [b], Mani Outis [b], João C. Lima [b], Nuno Basílio [b], Victor de Freitas [a], Fernando Pina [b,**]

[a] LAQV – REQUIMTE, Departamento de Química e Bioquímica, Faculdade de Ciências, Universidade do Porto, Rua do Campo Alegre, 687, 4169-007, Porto, Portugal
[b] LAQV – REQUIMTE, Departamento de Química, Faculdade de Ciências e Tecnologia, Universidade Nova de Lisboa, 2829-516, Caparica, Portugal

ARTICLE INFO

Keywords:
Bis-aminostyrylbenzopyrylium derivative
B4 adduct
Stopped-flow
pH jumps

ABSTRACT

The kinetics and thermodynamics of the compound 7-diethylamino-2-(4′-dimethylaminostyryl)-1-benzopyrylium was studied in ethanol:water (1:1) and in microheterogenous media (SDS and CTAB micelles) and compared with its corresponding flavylium (7-diethylamino-4′-dimethylaminoflavylium) also known as 7-diethylamino-2-(4′-dimethylaminophenyl)-1-benzopyrylium. The introduction of a double bond between the benzopyrylium system and the phenyl group gives rise to vivid color changes resulting from the formation of violet protonated styrylbenzopyrylium cation (AH_2^{2+}), green styrylbenzopyrylium cation (AH^+), orange *trans*-chalcone (Ct) and magenta anionic *trans*-chalcone (Ct^-). All species except protonated styrylbenzopyrylium cation are stable for long periods.

In ethanol:water the pH domain of the styrylbenzopyrylium cation and *trans*-chalcone are respectively $\Delta pH = 4.5$ and 4.4 and the anionic *trans*-chalcone for pH > 10.5. In the presence of SDS micelles, there is an increase of the pH domain of the styrylbenzopyrylium cation $\Delta pH = 5.9$ at the expense of the *trans*-chalcones, $\Delta pH = 2.95$, while in CTAB it is the *trans*-chalcone the dominant species, $\Delta pH = 6.2$, with concomitant decreasing of the styrylbenzopyrylium cation pH range $\Delta pH = 1$. This can be due to the electric charge present on the surface of each micelle, for instance the negative charge surface of SDS micelles stabilizes the positive charge of styrylbenzopyrylium cation and its protonated form, while the positive charge surface of CTAB micelles stabilizes the negative and neutral charge of the *trans*-chalcones species.

The peculiar behavior of the kinetics in basic medium was investigated by stopped-flow. It was verified that in ethanol:water, SDS and CTAB micelles a transient species resulting from the OH^- attack to position 4 of the styrylbenzopyrylium cation (B4) behaves as a kinetic product delaying the kinetic toward the equilibrium.

1. Introduction

With a few exceptions, for example flavylium cations bearing an alkyl substituent in position 4, or pyranoflavylium compounds [1], synthetic flavylium cations generate a network of chemical species that is essentially the same observed in anthocyanins, exemplified in Scheme 1 for malvidin 3-*O*-glucoside, Scheme 1a.

These networks generated by flavylium cation are reversibly interconnected by external stimuli, in particular pH, but also light and temperature [1]. The flavylium cation is the stable species in acidic medium, in anthocyanins for $pH \leq 1$. Addition of base to the flavylium cation (direct pH jumps) triggers in anthocyanins a sequence of three kinetic processes that for final pH values in acidic medium are well separated in time. Proton transfer (sub microseconds) [3,4], hydration followed by a faster tautomerization, (seconds to minutes) and finally the much slower isomerization (hours). In the direct pH jumps to the basic medium, the isomerization is much faster than the OH^- nucleophilic addition and only a second step is observed, which is controlled by this last process. Between the acidic and basic paradigms there is a pH region where after a direct pH jump the quinoidal bases immediately formed decompose faster than hydration and OH^- nucleophilic addition [2].

Beyond the multiple functions of anthocyanins in biological systems and practical applications in these fields [1,5,6], the use of these natural compounds in other chemistry or materials science domains, faces a

* Corresponding author.
** Corresponding author.
E-mail addresses: jsoliveira@fc.up.pt (J. Oliveira), fp@fct.unl.pt (F. Pina).

https://doi.org/10.1016/j.dyepig.2024.112280
Received 1 February 2024; Received in revised form 6 June 2024; Accepted 11 June 2024
Available online 12 June 2024

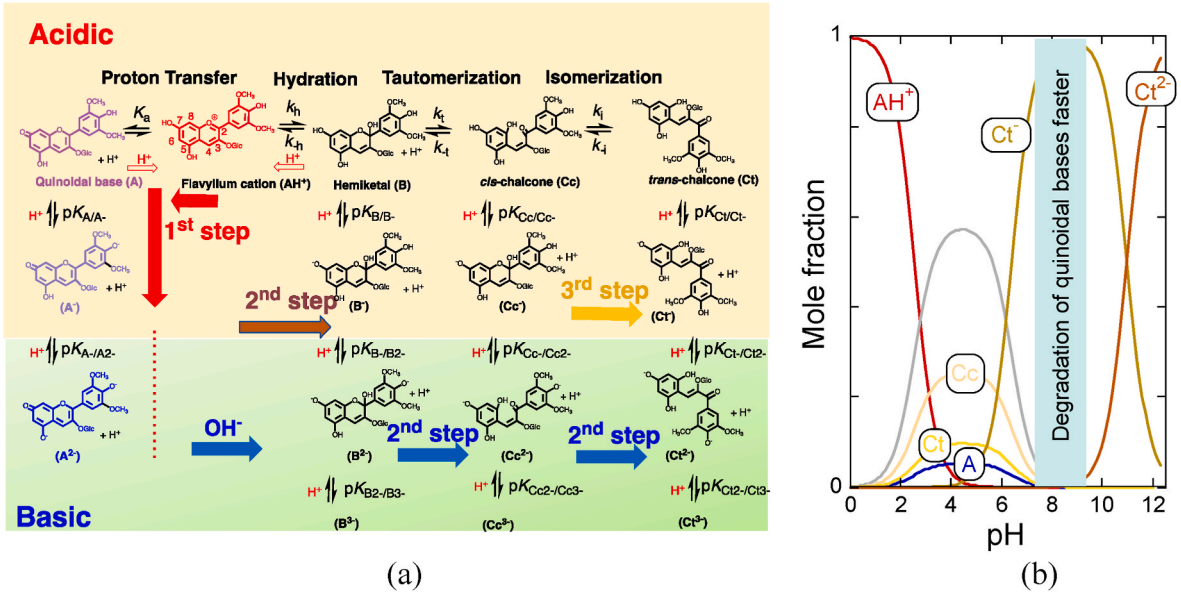

Scheme 1. **(a)** Network of chemical species of malvidin 3-*O*-glucoside; **(b)** mole fraction distribution of malvidin 3-*O*-glucoside at the equilibrium. This scheme is also observed for synthetic flavylium systems. In the case of anthocyanins, there is a pH region where after a direct pH jump the anionic quinoidal bases immediately formed decompose faster than hydration and OH^- nucleophilic addition [2].

severe drawback: their instability. However, it is possible to profit from this complex network of species, by means of synthetic flavylium compounds. The number of these molecules already reported is very high as well as the possibility of preparing new ones. In any flavylium-based systems, for each network species, Scheme 1b, its color, pH domain and stability are dramatically dependent on the nature and position of the substituents.

In the sixties of the last century, Jurd claimed in a patent [7] that the instability of anthocyanins is primarily due to the substituents in position 3 and stability is achieved provided that hydrogen, lower alkyl, phenyl, alkoxy and phenoxy are used. On this line, Matsushima et al. [8, 9] and Tron et al. [10] reported amine substituents in positions 7 and 4′ of the flavylium cation. Except in very acidic solutions for the protonated flavylium cation, this substitution pattern gives rise to the stability of the network species in an extended pH region, including the basic one, and intense blue flavylium cations, Scheme 1.

In a previous paper [11] we compare the effect of the solvent conditions, Water/Ethanol (1:1), SDS and CTAB micelles on the pH domain of the species reported in Scheme 2, for 7-Diethylamino-4′-dimethylaminoflavylium. Dramatic effects on the pH domain of the several species were observed. Moreover, the number of the observed species at the equilibrium is very simplified in basic medium, pH > 13, only flavylium cation (including its protonated form at extremely acidic pH values) and *trans*-chalcones (di-protonated, mono-protonated, neutral and anionic) were detected, Scheme 2.

In the same patent by Jurd [7], styrylbenzopyrylium compounds are described with the aim of obtaining deeper hues. These facts prompted us to synthesize the *bis*-aminostyrylbenzopyrylium compound shown in Scheme 3b.

One of the objectives of this work is to investigate the effect of the introduction of the styryl group over the phenyl group on the stimuli response of compounds and on the modification of the color's pallet of the different species of the network.

While *bis*-aminoflavylium cations are blue, the question was if extending the π-π conjugation it would be possible to get green styrylbenzopyrylium cations. Another question was to account for the kinetic pathways that convert styrylbenzopyrylium cation in anionic *trans*-chalcone, particularly for pH > 13 and profit from the use of stopped-flow to monitor the fast kinetic steps upon pH jumps, which are not accessed by means of a standard spectrophotometer.

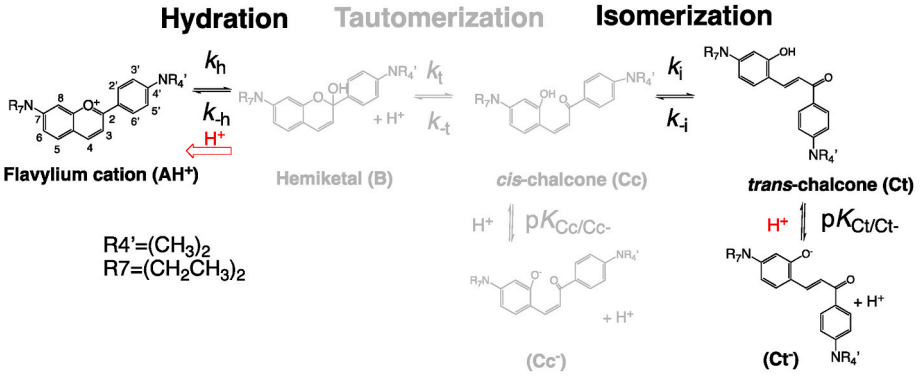

Scheme 2. General kinetic scheme of the chemical species generated by *bis*-aminoflavylium cation. The species in grey are transients generally not directly detected in this system, except for colorless species in basic medium [12]. Flavylium cation can protonate in very acidic conditions and transient mono and di-protonated *trans*-chalcones can be observed. For pH > 13 there is spectral evidence for the formation of colorless transients.

2. Results and discussion

2.1. Ethanol:water

2.1.1. Direct pH jumps

In Fig. 1 the spectral variations at the equilibrium of the compound BisNStB, 3.8×10^{-5} M, upon a series of pH jumps from equilibrated flavylium cation in ethanol:water (1:1) are presented. Inspection of these figures indicates that styrylbenzopyrylium cation can protonate at very acid solutions, Fig. 1a, and equilibrate with *trans*-chalcone, in moderately acidic medium, Fig. 1b. The anionic *trans*-chalcone is observed for higher pH values, Fig. 1c. In this way the behavior of the styryl derivative is like the equivalent flavylium cation, BisNF. The protonated styrylbenzopyrylium cation degrades after several days. The titration curves at three representative wavelengths allow for the determination of the respective acid-base constants, Fig. 1d.

When the pH domain of the species observed in BisNStB and the respective colors are compared with those of 7-Diethylamino-4′-Dimethylaminoflavylium (BisNF), Fig. 2, all species of the *bis*-aminostyrylbenzopyrylium exhibit a significant red shift in the respective absorption bands, the highest difference occurring for the styrylbenzopyrylium cation, Fig. 2a and b. Concerning the acidity constants, the highest difference occurs for the protonation of the styrylbenzopyrylium cation. This is an expected result since the amine substituent in position 4′ is farther from the positive charge of ring C in the styryl compound, decreasing the electrostatic repulsion and making protonation easier. The most dramatic change is however the perception of the colors of all observed species, see below Scheme 5. It is worth noting the green colors of the styrylbenzopyrylium cation and magenta of the anionic *trans*-chalcone.

The absorption spectra of the styrylbenzopyrylium cation in its large pH domain (1.6<pH < 6.1) do not change significantly after 7 days, in

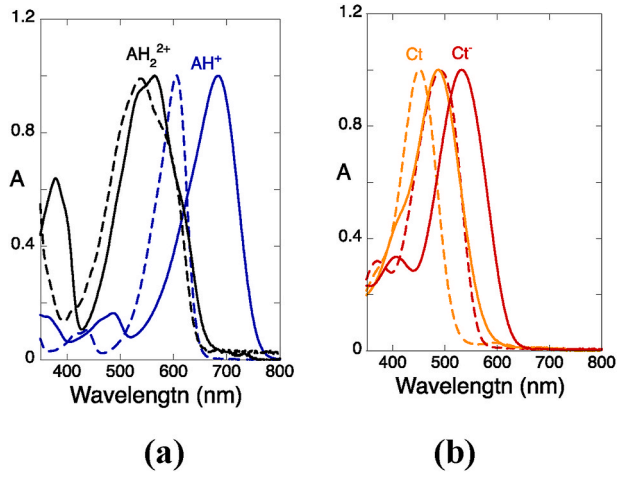

Fig. 2. **(a)** Comparison between the absorption spectrum of the cationic form (AH^+) and its protonated form (AH_2^{2+}) (full line the styryl compound, traced line the related flavylium); **(b)** the same for neutral (Ct) and anionic *trans*-chalcones (Ct^-).

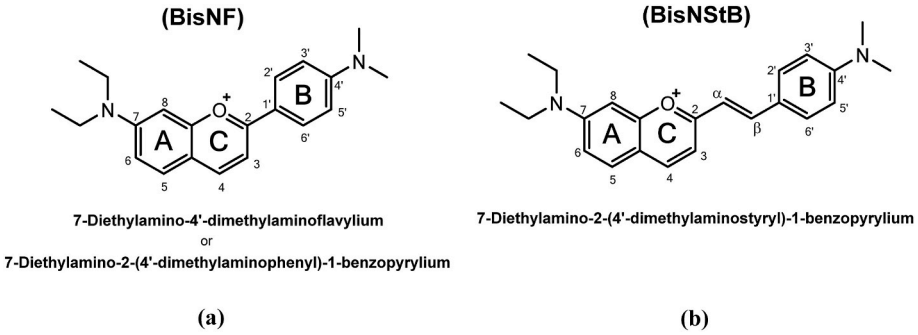

Scheme 3. **(a)** *Bis*-aminoflavylium (BisNF) and **(b)** *Bis*-aminostyrylbenzopyrylium (BisNStB).

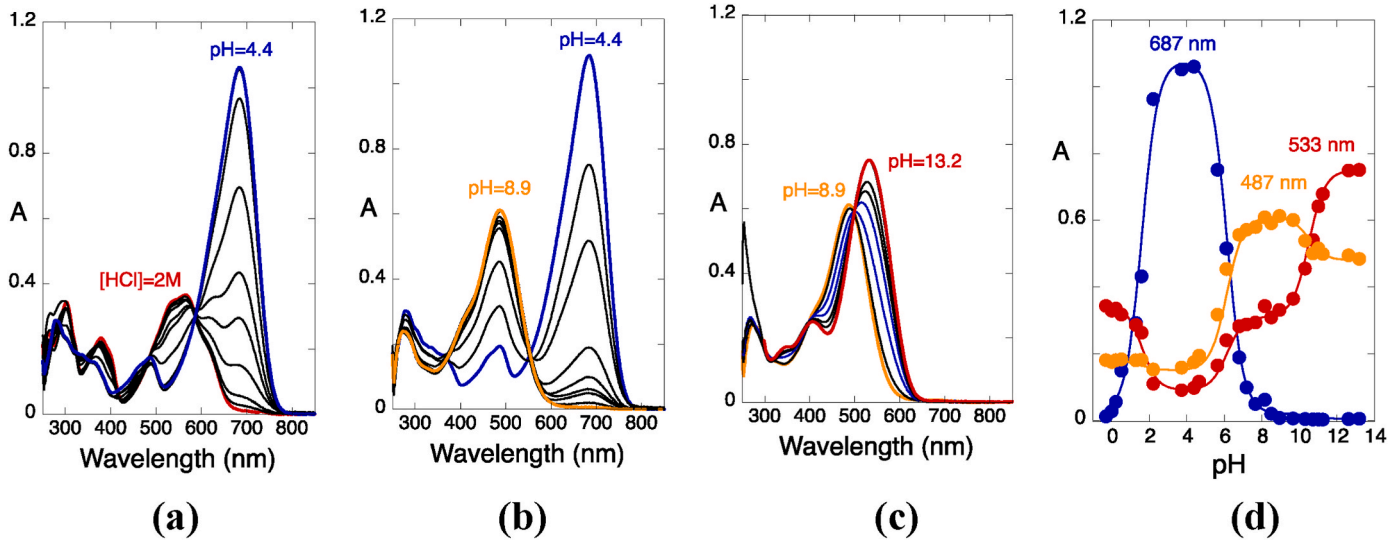

Fig. 1. Spectral variations of BisNStB (3.8×10^{-5} M), in the ethanol:water (1:1) at the equilibrium after a series of pH jumps from equilibrated styrylbenzopyrylium cation; **(a)** equilibrium between AH_2^{2+} and AH^+ achieved for p$K = 1.6$; **(b)** equilibrium between AH^+ and Ct p$K = 6.1$; **(c)** equilibrium between Ct and Ct^- p$K = 10.5$; **(d)** Titration curves at three representative wavelengths.

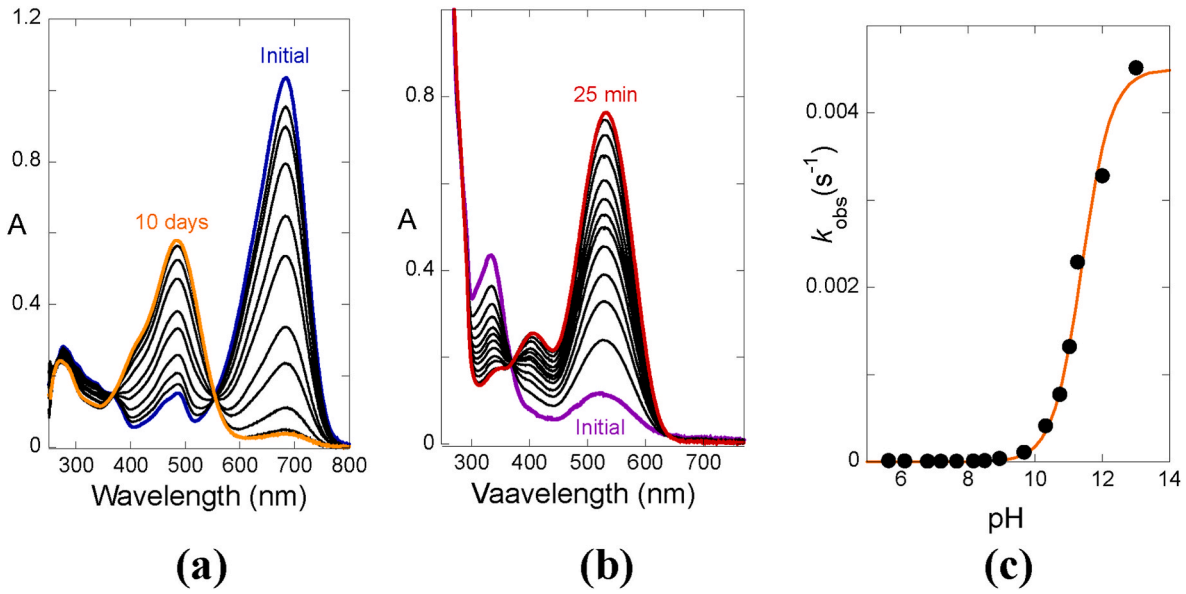

Fig. 3. Spectral variations after a direct pH jump of BisNStB (3.8×10^{-5} M) **(a)** to pH = 7.7; **(b)** to pH = 13.2.; **(c)** representation of the rate constants after direct pH jumps toward the equilibrium.

contrast with its protonated form which is unstable.

The spectral variations after a direct pH jump to the basic region are represented in Fig. 3a and b. The styrylbenzopyrylium cation disappears slowly at pH 7.7 to give the *trans*-chalcone. The presence of isosbestic points suggests that the species that necessarily are involved in the conversion of styrylbenzopyrylium cation to *trans*-chalcone are transients, not observed directly. This behavior is like the kinetics of 3-deoxyanthocyanins in basic to neutral medium, where hemiketal (B2) and *cis*-chalcone are not observed (once formed disappear to give the respective *trans*-chalcone) [13].

A direct pH jump to pH 13.2 is different. The disappearance of the styrylbenzopyrylium cation is not observed in the time scale required to collect a spectrum by the standard spectrophotometer. The initial spectrum possesses an absorption band that is the same as the final spectrum identified as the anionic *trans*-chalcone and there is another band that can be attributed to colorless species. The question is: Why in Fig. 3b the anionic *trans*-chalcone is partially formed at a very fast rate, but the system takes circa 25 min to reach the equilibrium (constituted by the same anionic *trans*-chalcone)?

2.1.2. *Kinetics monitored by stopped flow. The B4 hypothesis*

More information regarding the direct pH jumps to pH > 13 was obtained by monitoring the direct pH jumps by stopped-flow, Fig. 4.

As will be described below, the photochemistry of the chalcones is very inefficient but there is the possibility of the light interference in the transient species absorbing in the UV region of the spectrum. Due to the high intensity of the stopped-flow analyzing lamp a cutoff filter of 425 nm was used, to prevent this possibility. Inspection of Fig. 4a shows a very fast disappearance of the styrylbenzopyrylium cation. After 0.1 s a transient equilibrium between styrylbenzopyrylium cation (minor species) and other eventual species not absorbing in the visible (whose absorption spectra cannot be visualized due to the filter) is reliable. In a second kinetic step, another transient equilibrium is achieved, with the absorption spectrum after 100 s coincident with the one of the anionic *trans*-chalcone, the species present at the equilibrium at pH > 13, see Fig. 3b. The obvious colorless candidate in the first transient equilibrium with AH^+ after 0.1 s is the hemiketal B2 (in eventual equilibrium with Cc^-). It is worth noting that in basic medium the *cis-trans* isomerization is very fast, as already observed in anthocyanins [14]. This last assumption was confirmed by density functional theory (DFT) calculations of the *cis* → *trans* isomerization energy barriers. The anionic

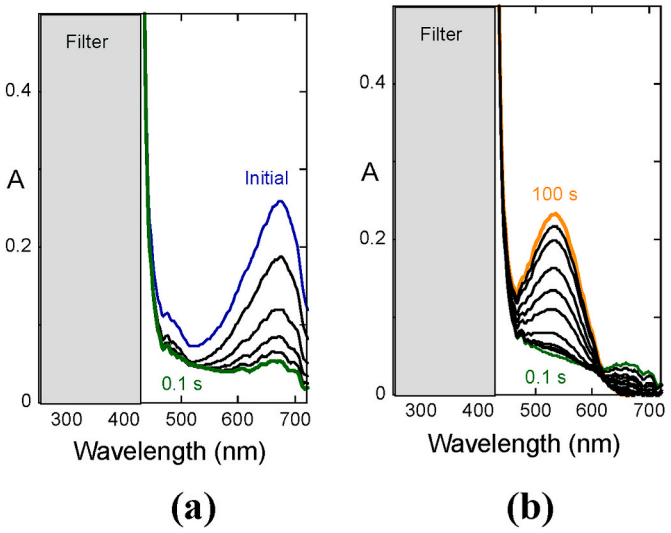

Fig. 4. **(a)** Spectral variations after a direct pH jump of BisNStB in ethanol: water to pH 13.6 in the presence of a cutoff filter 425 nm, monitored by stopped-flow, faster kinetic step; **(b)** the same for the slower kinetic step.

chalcone requires an activation energy of 23.7 kcal mol^{-1} while in the neutral form 40.8 kcal mol^{-1}. According to the Arrhenius equation, assuming a similar pre-exponential factor in the *cis-trans* isomerization mechanism of both anionic and neutral forms, the isomerization would be faster by a factor of 10^{13} in the anionic form. For more details see supplementary material.

Consequently, it can be understood that the anionic *trans*-chalcone is the species observed after 100 s. However, this situation does not represent the (final) equilibrium which is much slower as reported in Fig. 3c. In conclusion, the kinetic model represented by eq. (1) to eq. (3) does not account for the present kinetics.

$$AH^+ + OH^- \rightleftharpoons B2 \qquad K_{B2} \tag{1}$$

$$B2 \rightleftharpoons Cc^- \qquad K_{Cc-} \tag{2}$$

$$Cc^- \rightleftharpoons Ct^- \qquad K_{Ct-} \tag{3}$$

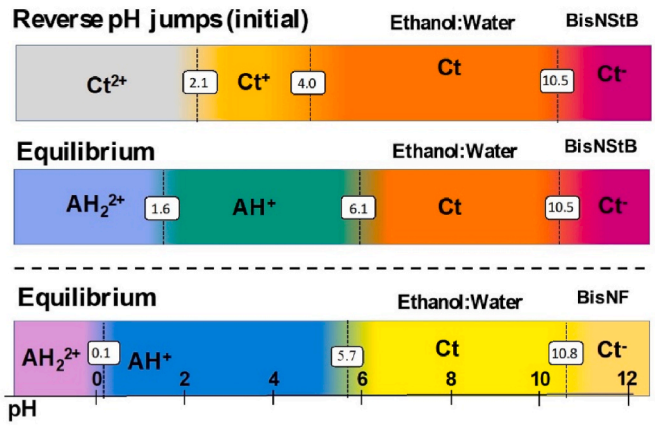

Scheme 4. pH domain of the *bis*-aminostyrylbenzopyrylium (BisNStB) in ethanol:water at the equilibrium and its flavylium parent (BisNF), down, and the pH domain of the reverse pH jumps of the *trans*-chalcones immediately after the jump.

An alternative model is to consider the formation of B4, eq. (4), Scheme 5.

$$AH^+ + OH^- \rightleftharpoons B4 \qquad K_{B4} \tag{4}$$

This model is inspired by previous work by McClelland and co-workers, who observed in the case of flavylium systems, lacking the hydroxyl substituents, formation of the adduct B4 resulting in the attack of water to the position 4 of the flavylium cation [12]. According to this alternative interpretation the spectral variations of Fig. 4a (hidden by the filter) would result from the formation of B2, and B4 by two parallel reactions followed by the equilibrium between B2 and Cc^-. In Fig. 4b all species of this first transient equilibrium (including AH^+) evolve to Ct^-, but B4 remains since it is a kinetic species that disappears to give the final species anionic *trans*-chalcone only via styrylbenzopyrylium cation. In other words, the rate of this slower process (presented in Fig. 3b) is a function of the mole fraction of styrylbenzopyrylium cation in its equilibrium with B4 (χ_{AH+}). As demonstrated in the appendix, the rate constant toward the equilibrium, Fig. 3c–is given by eq. (5).

$$k_{obs} = \chi_{AH+}\, k_{eq.}[OH^-] = \frac{k_{eq.}[OH^-]}{1 + K_{OH}[OH^-]} \tag{5}$$

Where $k_{eq.}$ is the rate constant of the OH^- nucleophilic addition to the styrylbenzopyrylium cation and K_{OH} is the equilibrium constant between styrylbenzopyrylium cation and all other species after the first step that gives the kinetic reservoir B4.

Eq. (5) could have two approximations: *i)* for very high concentration [OH^-] the observed rate tends to a plateau given by $k_{eq.}/K_{OH}$; *ii)* when the concentration of OH^- is not enough (as in the presence of SDS micelles) $K_{OH}[OH^-]$ could be $\ll 1$ and the observed rate given by, $k_{eq.}[OH^-]$.

In ethanol:water, fitting of the data of Fig. 3c was achieved for $k_{eq.} = 2\ M^{-1}\ s^{-1}$ and $K_{OH} = 444\ M^{-1}$

In the case of malvidin 3,5-*O*-diglucoside the chemical structure of $B4_4^{2-}$ was recently fully characterized by ^{1}H NMR [14]. While formation of $B4_4^{2-}$ is too fast to be monitored by ^{1}H NMR, its disappearance can be followed by lowering the temperature to 5 °C. For example, immediately after a direct pH jump to pH = 12.9, 80 % of $B4^{2-}$ is formed and its decay is sufficiently slow at this temperature to run several ^{1}H NMR spectra up to its total disappearance.

2.1.3. Reverse pH jumps

The reverse pH jumps were performed from anionic *trans*-chalcone at pH = 12.6 to lower pH values and monitored by stopped-flow.

Fig. 5a reflects the equilibrium between the di and mono-protonated *trans*-chalcones mixed with the equilibrium between protonated *trans*-chalcone and neutral *trans*-chalcone. Due to the similarity of the absorption spectra of Ct^+ and Ct, it is not possible to clearly separate the two equilibria. Fig. 5b shows the equilibrium between neutral *trans*-chalcone and anionic *trans*-chalcone. The titration curves at three representative wavelengths allow for the determination of the respective acid base constants p*K*s 2.1, 4.0 and 10.5, Fig. 5c.

The results are summarized in Scheme 5.

According to Scheme 5, chalcones are the equilibrium species for pH values from neutral to basic. pH jumps in this range are unable to change the color. In acidic medium after a reverse pH jump the chalcones give spontaneously the styrylbenzopyrylium cation or its protonated form depending on the final pH.

2.2. SDS micelles

2.2.1. Direct pH jumps

The spectral variations after a pH jump from equilibrated solutions of the styrylbenzopyrylium cation at pH = 5.1 in the presence of SDS micelles (0.1 M) upon the addition of acid are shown in Fig. 6a. The full lines represent the absorption spectra obtained immediately after addition of acid. The protonation of the styrylbenzopyrylium cation leading, AH_2^{2+}, occurs for pK = 3, which compares with pK = 1.6 in ethanol:water (1:1). Again, the protonated styrylbenzopyrylium cation is not stable. A series of pH jumps to the pH domain of AH_2^{2+}, was carried out and the absorption spectra collected after 6 days were plotted in Fig. 6a and b, traced lines. The fact the protonated styrylbenzopyrylium cation is not stable was confirmed by the addition of base to the solution at pH = 1.2 (after 6 days) to achieve pH circa 7. No recovery of any styrylbenzopyrylium cation was observed. Since the initial absorption spectra are coincident in all very acidic pH region there is no evidence for the protonation of the second amino substituent. The pH-dependent absorption spectra in the pH region 1.2<pH < 7.6 taken immediately after the pH jumps, Fig. 6b full lines, clearly indicate the existence of an equilibrium between styrylbenzopyrylium cation and its protonated species. The spectral variations at the equilibrium between

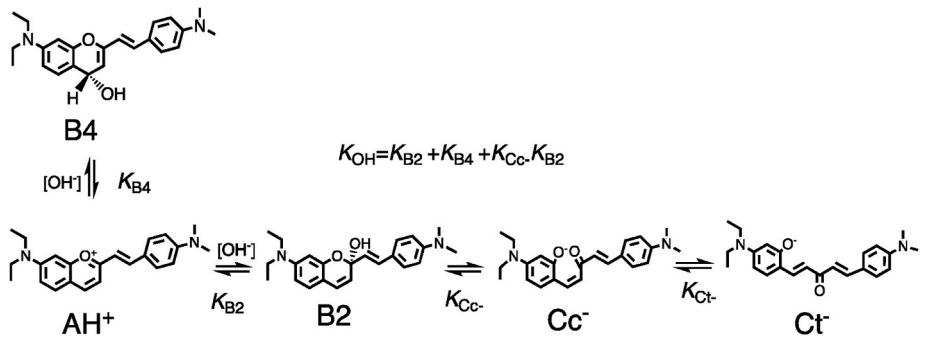

Scheme 5. Alternative model based on the formation of B4, see appendix.

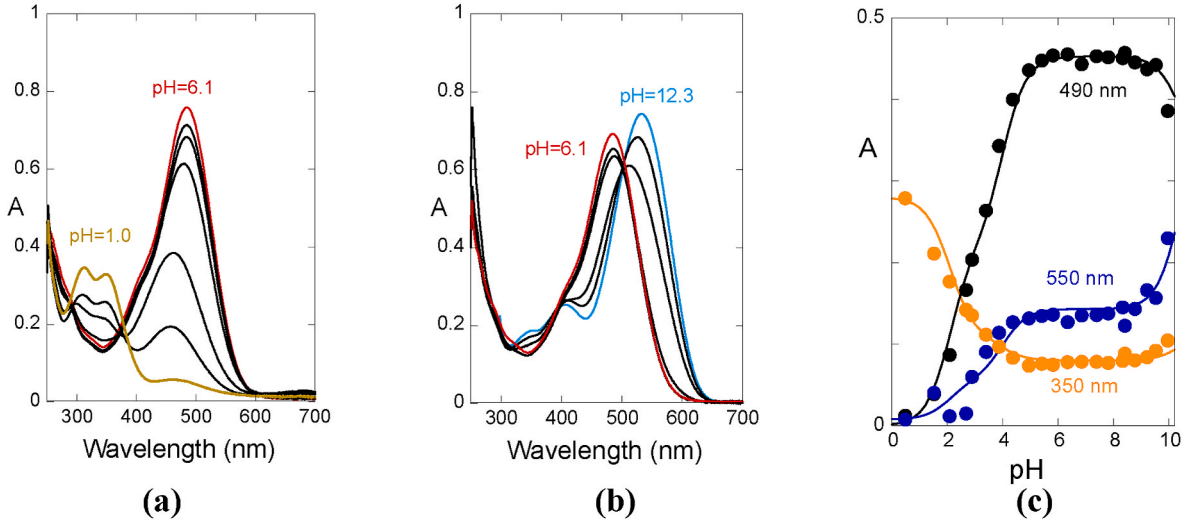

Fig. 5. Spectral variations of BisNStB ($3.8x10^{-5}$ M) after a series of reverse pH jumps taken immediately after the addition of acid **(a)** there are two p*K*s, Ct^{2+}/Ct^{+} and Ct^{+}/Ct whose absorption spectra cannot be clearly separated; **(b)** Ct/Ct; **(c)** titration curves at three representative wavelengths.

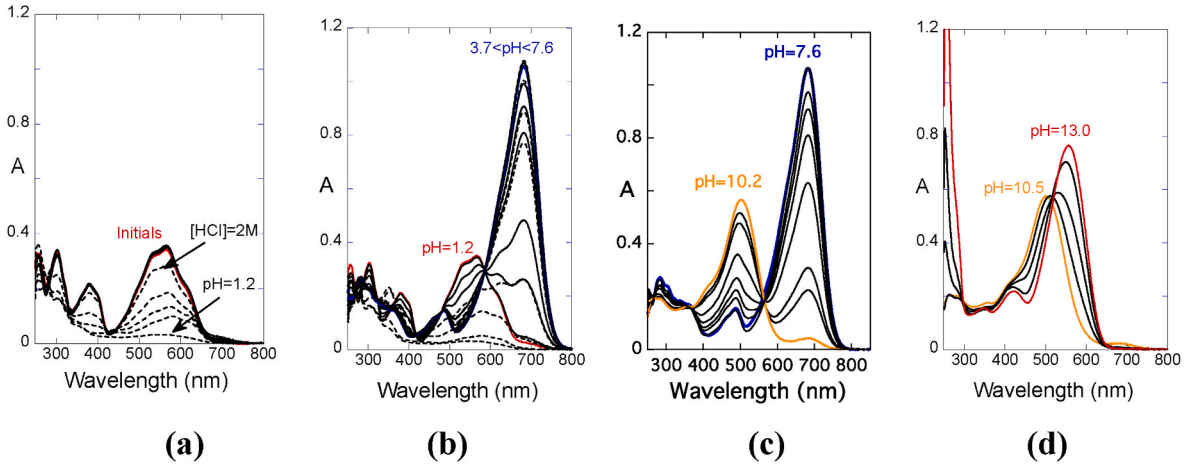

Fig. 6. Spectral variations after a direct pH jump of BisNStB (4.2×10^{-5} M) in the presence of SDS micelles (0.1 M) at the equilibrium. Traced lines after 6 days in very acidic medium: **(a)** in extremely acidic medium; **(b)** 1.2<pH < 7.6; **(c)** 7.6<pH < 10.2; **(d)** 10.5<pH < 13.

styrylbenzopyrylium cation and *trans*-chalcone and between this last one and its anionic form are shown respectively in Fig. 6c and d.

When Fig. 6 is compared with the system in ethanol:water, Fig. 1, it can be concluded that the color of both network species is very similar, but the respective pH domain changes dramatically.

In Fig. 7 the mole fraction distribution of all species in the presence of SDS micelles at the equilibrium is reported. Due to the degradation of the protonated styrylbenzopyrylium cation the acidity constant between this species and styrylbenzopyrylium cation, pK = 3, was calculated from absorption spectra taken immediately after the pH jump. For the other species the following equilibrium constants between styrylbenzopyrylium cation and *trans*-chalcone, pK = 8.85, and *trans*-chalcone and its anionic form, pK = 11.8, were calculated.

The spectral variations taking place in basic medium are illustrated in Fig. 8a. Initially the styrylbenzopyrylium cation is formed and evolves to the *trans*-chalcone or its anionic form to more basic solutions. The fact that the isosbestic point is red-shifted from Fig. 8a to b is a consequence of the formation of the anionic *trans*-chalcone in the last.

As shown below, there is experimental evidence by stopped-flow that B4 is also formed. However, the inflection point and the plateau predicted by eq. (5) are not observed. On the other hand, it is not possible to increase the OH^- concentration because precipitation occurs after a few minutes. Due to the negative charge of the SDS micelles surface the

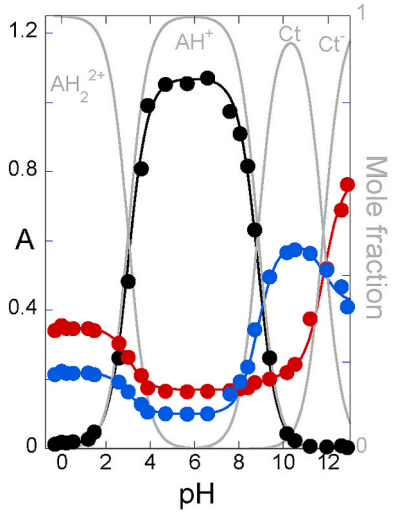

Fig. 7. Mole fraction distribution of BisNStB (4.2×10^{-5} M) in the presence of SDS micelles (0.1 M). Fitting was achieved for the equilibrium between AH_2^{2+}/AH^+, pK = 3; AH^+/Ct, pK = 8.85; and Ct/Ct^-, pK = 11.8.

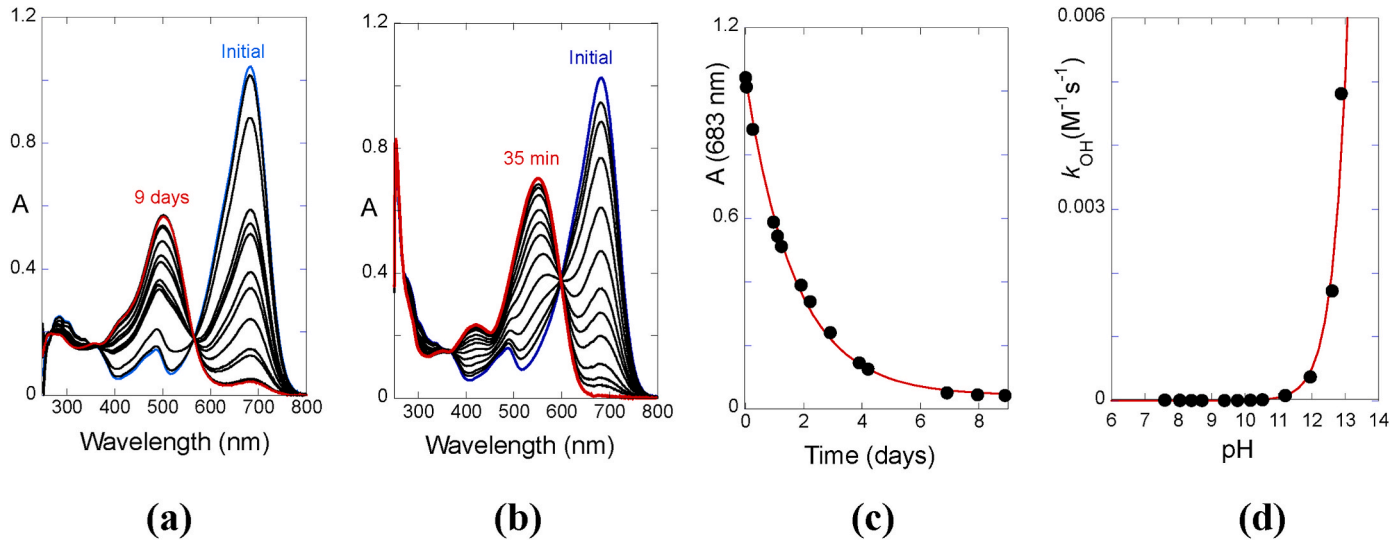

Fig. 8. **(a)** Spectral variations of BisNStB (4.2×10^{-5} M) in the presence of SDS micelles (0.1 M), after a direct pH jump from styrylbenzopyrylium cation to pH = 10.2; **(b)** The same of (a) for pH = 12.6; **(c)** kinetic trace of the absorbance at 683 nm for pH = 10.2. Fitting was achieved with a mono-exponential $k_{obs} = 6.85 \times 10^{-6}$ s^{-1}; **(d)** rate constant of the flavylium cation disappearance in basic medium. Fitting was achieved by means of eq. (5), for $k_{eq} = 0.05$ $M^{-1}s^{-1}$. The inflection toward a plateau was not achieved in this pH range.

effective concentration of OH^- is much less than the one corresponding to the pH of the bulk solution. Fitting was achieved for $k_{eq} = 0.05$ $M^{-1}s^{-1}$ by means of the second approximation of eq. (5) above reported ($k_{obs} = k_{eq.}[OH^-]$).

2.2.2. *Reverse pH jumps*

A series of reverse pH jumps to determine the acid-base constants of the chalcones is reported in Fig. 9. The similarity of the absorption spectra of Ct^+ and Ct prevents a clear visualization of the respective isosbestic points and consequently the absorption spectra of the two processes are presented together, Fig. 9a. Fig. 9b shows the equilibrium between neutral *trans*-chalcone and anionic *trans*-chalcone. Titration curves at three representative wavelengths are presented in Fig. 9c. Fitting was achieved for p$K = 2.1$ between Ct^{2+}/Ct^+, p$K = 5.0$ for Ct^+/Ct and 11.8 for Ct/Ct^-.

2.2.3. *Stopped-flow*

In Fig. 10 the spectral variations of BisNStB in the presence of SDS micelles after a direct pH jump to pH = 12.9 monitored by stopped-flow are presented. Fig. 10a–c were collected without any cutoff filter, while in Fig. 10d and e, a cutoff filter of 425 nm was used. A comparison of the two kinetics could also give some information regarding the photochemical behavior of the transient species.

The stopped-flow experiments with filter are compatible with the model above presented in Scheme 4. After 2.5 s a transient equilibrium involving AH^+, B2 (*Cc*-) and B4 is established, Fig. 10d. The next step could be assigned to the flow of AH^+ and B2 (Cc^-) to give anionic *trans*-chalcone. B4 remains trapped in this time scale and retards the kinetics

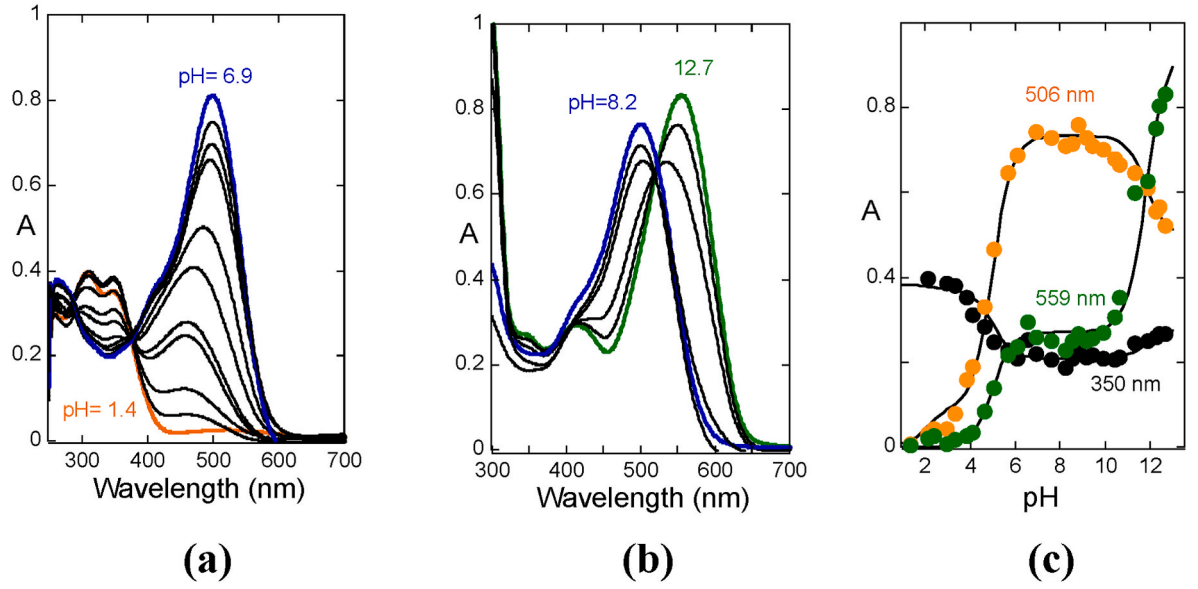

Fig. 9. Spectral variations upon a reverse pH jump from anionic *trans*-chalcone of BisNStB (4.2×10^{-5} M) in the presence of SDS micelles (0.1 M); **(a)** spectral variations corresponding like in Fig. 5a to the two protonations of the *trans*-chalcones; **(b)** spectral variations regarding the acid-base equilibrium between *trans*-chalcone and its anionic species; **(c)** titration curves at three representative wavelengths. Fitting was achieved for p$K = 2.1$ between Ct^{2+}/Ct^+, p$K = 5.0$ for Ct^+/Ct and 11.8 for Ct/Ct^-.

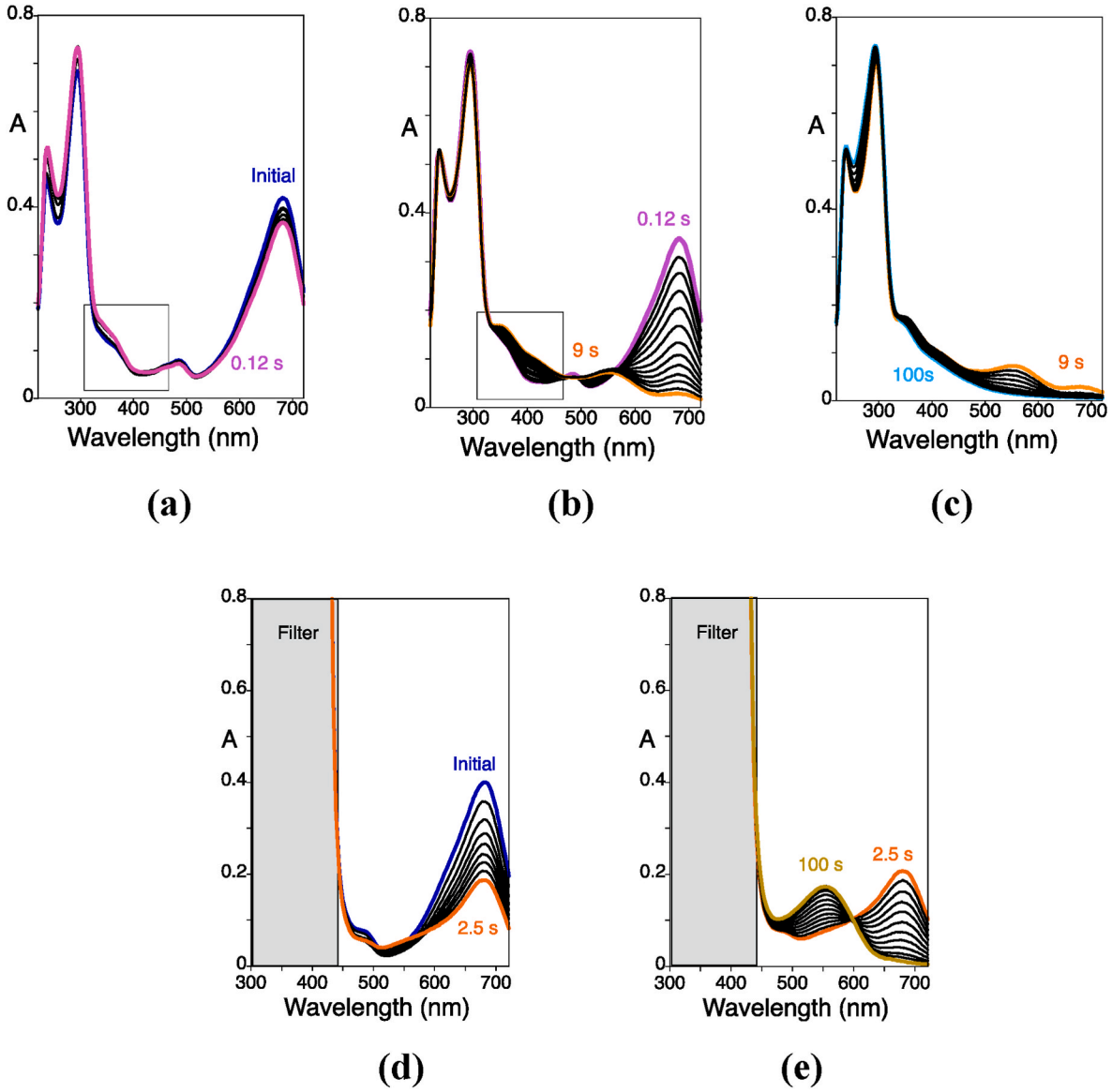

Fig. 10. Spectral variations of BisNStB (4.2×10^{-5} M) in the presence of SDS micelles (0.1 M) after a direct pH jump to pH = 12.9 monitored by stopped-flow; **(a)** to **(c)** in the absence of cutoff filter; **(d)** and **(e)** with a cutoff filter of 425 nm.

toward the new equilibrium.

Some information regarding the photo-induced reactions of the transient species can be achieved by comparing the spectral variations in the presence and absence of the cutoff filter. In the absence of the filter the styrylbenzopyrylium cation disappears faster. Light promotes a reaction that restores styrylbenzopyrylium cation. A possible explanation is the previously described light induced opening of the hemiketal [15]. Under light no anionic *trans*-chalcone is formed after 100 s in comparison with Fig. 10e.

Scheme 6 summarizes the acid-base constants in the presence of SDS. Comparison of the pH domain of styrylbenzopyrylium with the analog flavylium shows again a similitude with the acidity constants in basic medium and a great difference in the protonation of the cationic form (AH_2^{2+}).

In SDS the pH domain of the *trans*-chalcone is reduced and the chalcones upon direct pH jumps give spontaneously the styrylbenzopyrylium cation or its protonated form for all acidic and slightly basic pHs.

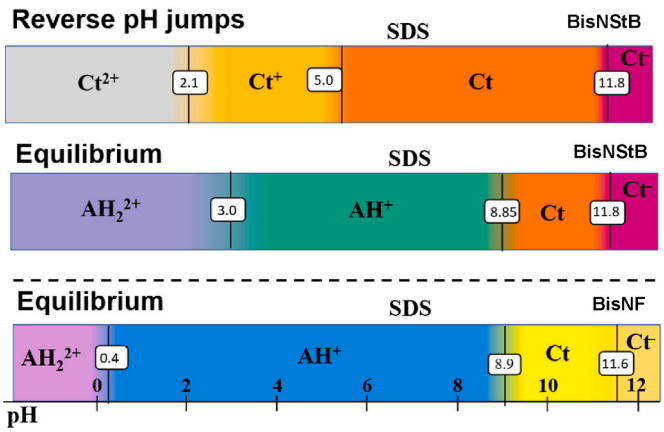

Scheme 6. pH domain of BisNStB in SDS micellles at the equilibrium and its flavylium parent (BisNF), down, and the pH domain of the reverse pH jumps of the *trans*-chalcones immediately after the jump.

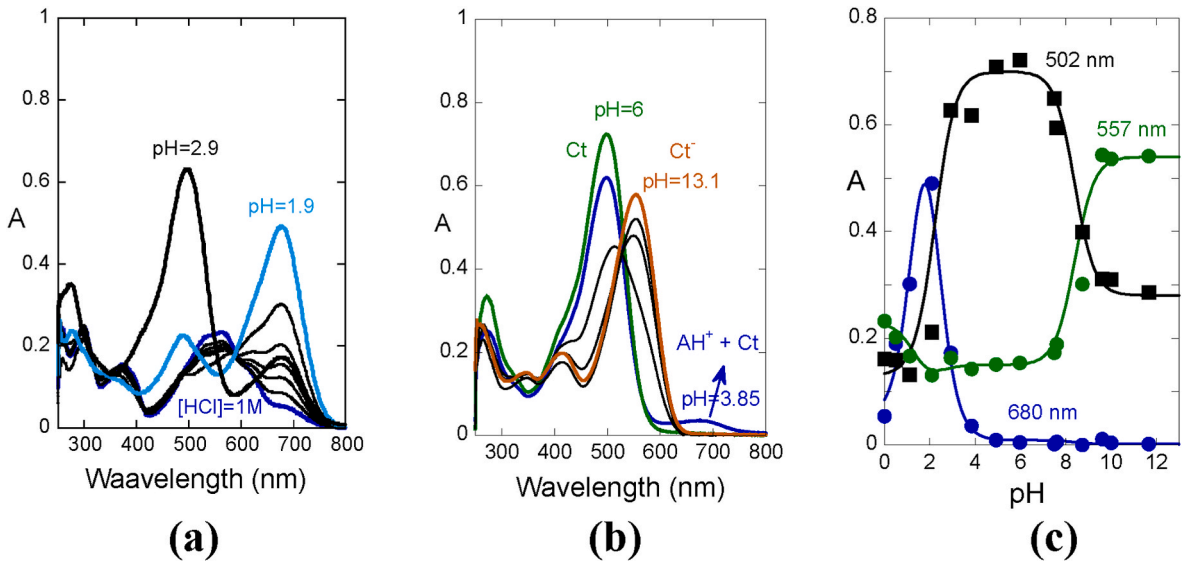

Fig. 11. Spectral variations of BisNStB (4.2×10^{-5} M) in the presence of CTAB micelles (0.1 M); **(a)** protonation equilibrium between styrylbenzopyrylium cation and its protonated form; **(b)** spectral variations referring to the deprotonation of the *trans*-chalcone. The acid-base constants regarding the protonation of the styrylbenzopyrylium cation and the equilibrium between this last and *trans*-chalcone are close and the two processes mixture preventing the appearance of isosbestic points in the pH range 2.1<pH < 4; **(c)** Titration curves at the equilibrium for three representative wavelengths. Fitting was achieved for $pK_{AH22+/AH+} = 1.3$; $pK_{AH+/Ct} = 2.3$; $pK_{Ct/Ct-} = 8.5$.

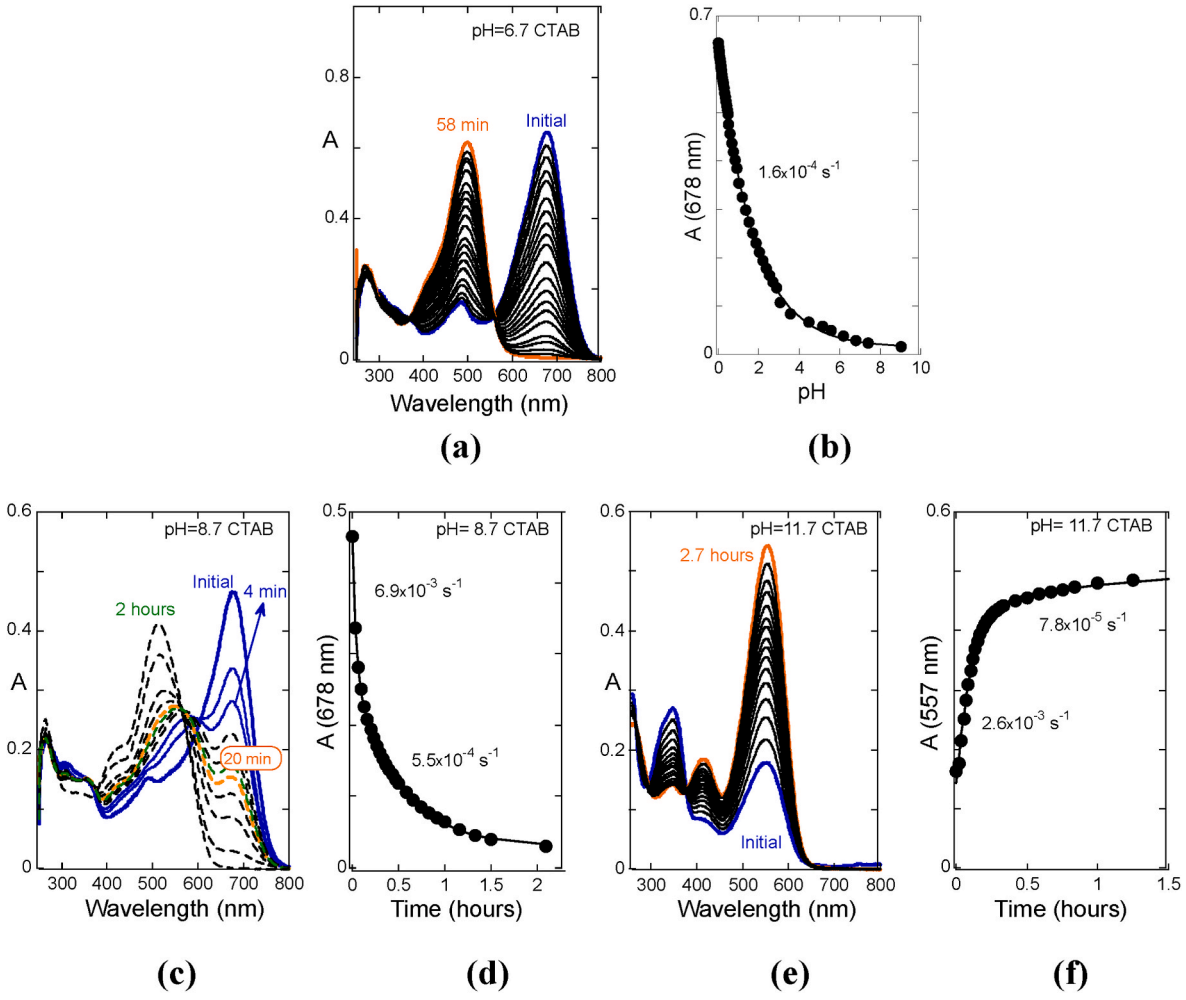

Fig. 12. **(A)** Spectral variations of BisNStB (4.2×10^{-5} M) in the presence of CTAB micelles (0.1 M), after a direct pH jump to pH = 6.7; **(b)** trace at 678 nm. Fitting was achieved with a mono-exponential of rate constant 1.6×10^{-4} s^{-1}; **(c)** The same of (a) for pH = 8.7.; **(d)** Trace of (c) at 678 nm. Fitting was achieved with a bi-exponential rate constants 6.9×10^{-3} s^{-1} and 5.5×10^{-4} s^{-1}; **(e)** The same of (c) for pH = 11.7; **(f)** Trace of (e) at 557 nm. Fitting was achieved for 2.6×10^{-3} s^{-1} and 7.8×10^{-5} s^{-1}.

2.3. CTAB micelles

2.3.1. Direct pH jumps

The spectral variations of BisNStB (4.2×10^{-5} M) in the presence of CTAB micelles at the equilibrium after a series of direct pH jumps are shown in Fig. 11. The acid base constant for the protonation of the styrylbenzopyrylium cation (leading to an unstable form) pK = 1.3 and the equilibrium between styrylbenzopyrylium cation and *trans*-chalcone pK = 2.3 are close preventing a clear definition of isosbestic points as observed above in Fig. 9a.

In Fig. 12 the kinetics toward the equilibrium after a direct pH jump are presented. Considering the equilibrium between neutral and anionic *trans*-chalcone pK = 8.5, the spectral variations at three representative pH values were selected: *i)* pH = 6.7 where only neutral chalcones are involved, *ii)* pH = 8.5 corresponding to a mixture of neutral and anionic chalcones; *iii)* pH = 11.7 only anionic chalcones are involved.

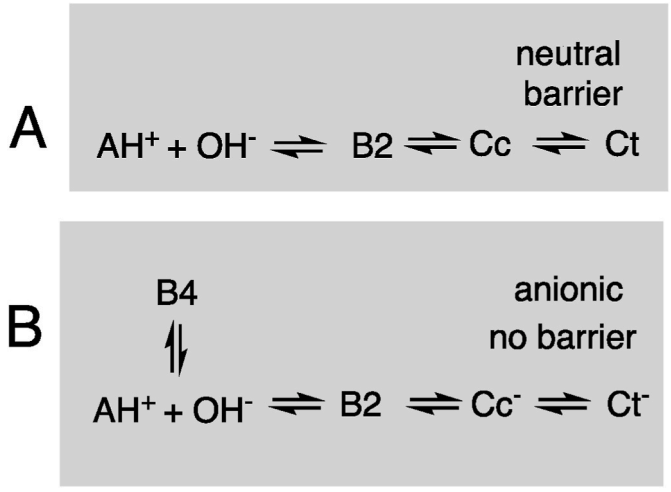

Scheme 7. First kinetic steps when neutral chalcones or anionic chalcones are involved.

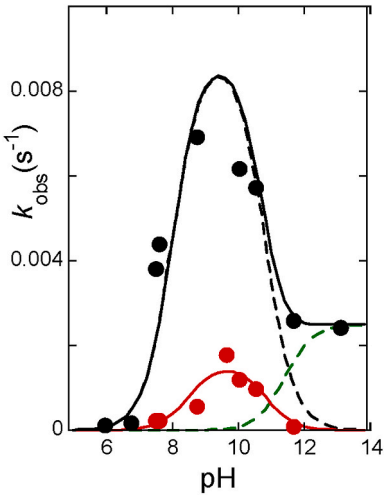

Fig. 13. Rate constants of BisNStB (4.2×10^{-5} M) in the presence of CTAB micelles (0.1 M) after direct pH jumps as shown in Fig. 10. Fitting was achieved considering the equilibrium between AH^+, *Cc* and Cc^- for a $pK_{AH+/Ct} = 8.5$; $pK_{Cc/Cc-} = 10.8$ (bell shaped contribution) and another contribution applying eq. (5) $k_{eq.} = 1\ s^{-1}M^{-1}$, $K_{OH} = 400\ M^{-1}$ (traced green line).

In the case of a direct pH jump to pH = 6.7, the styrylbenzopyrylium cation gives directly the *trans*-chalcone with isosbestic points and mono-exponential kinetics. This behavior presupposes that B2 and *Cc* are transient species and is illustrated in Scheme 7A. In contrast, the spectral variations after a direct pH jump to pH = 11.7, Fig. 12e as well for higher pH values, show the almost total disappearance of the styrylbenzopyrylium cation at the initial spectrum requiring the use of the stopped-flow for the determination of the respective kinetics, see below. The anionic *trans*-chalcone is already present at the initial spectrum. In scheme 7B the first kinetic step after direct pH jumps to the basic region is schematized. As observed in anthocyanins the *cis-trans* isomerization in basic medium is very fast (in contrast with the neutral chalcones). In Fig. 12e since the initial time, the absorption spectrum of the anionic *trans*-chalcone is already observed. The question is why it takes almost 3 h to reach the equilibrium (mainly anionic *trans*-chalcone). The hypothesis is again the formation of the B4 species, that retards the kinetics toward the equilibrium, see below the stopped-flow studies.

Finally, at pH = 8.7 there is a mixture of the two kinetics, and it is possible to observe the fast process of the styrylbenzopyrylium cation disappearance leading to a transient species compatible with the formation of a *cis*-chalcone and its disappearance to give the final anionic *trans*-chalcone.

In Fig. 13 the rates of the kinetic processes versus pH are represented. Inspection of this figure indicates that a fitting can be done considering the acid-base equilibrium between styrylbenzopyrylium cation, neutral and anionic *cis*-chalcones. The bell shape is proportional to the mole fraction of the neutral *cis*-chalcone in this last equilibrium. At higher pH values the system behaves as above reported, and can be fitted with eq. (5), the green curve for $k_{eq.} = 1\ M^{-1}\ s^{-1}$ and $K_{OH} = 400\ M^{-1}$. The ascending branch of the bell-shaped curve can be associated with the disappearance of styrylbenzopyrylium cation to give B2 (faster kinetics) leading to a type of "pseudo-equilibrium" as observed for anthocyanins in acidic medium, followed by a further kinetic step where styrylbenzopyrylium continues to disappear to give the final equilibrium product (*trans*-chalcone). The descending branch of the bell shape curve corresponds to the change of regime due to the formation of B4, accounted for by eq. (5).

2.3.2. Reverse pH jumps

The acid-base constant between diprotonated/protonated and protonated/neutral *trans*-chalcones occurs for very acidic solutions. At these pH values the conversion of the *trans*-chalcones (mono and diprotonated) is very fast and the absorptions immediately after the pH jump are represented. As observed in ethanol:water and SDS micelles the definition of the two first p*K*s has a great uncertainty due to the similarity of the absorption spectra of Ct^+ and Ct. Moreover, these two p*K*s in the presence of CTAB micelles are very close, Fig. 14a and b. The pK regarding the equilibrium Ct/Ct-is shown in Fig. 14c. A titration at two representative pH values is presented in Fig. 14d.

2.3.3. Stopped-flow

The spectral variations of BisNStB (4.2×10^{-5} M) monitored by stopped-flow upon a direct pH jump to pH = 13.7 is shown in Fig. 15. Due to the high intensity of the stopped-flow analyzing lamp, it was necessary to use a filter to prevent the photochemical processes, Fig. 15a. The decay of the flavylium cation is mono-exponential with a rate constant 31 s^{-1}. No other process was observed up to 100 s.

The information achieved in the stopped-flow experiments indicates that the equilibrium between the colorless species and styrylbenzopyrylium cation is extremely fast. The absorption spectrum after

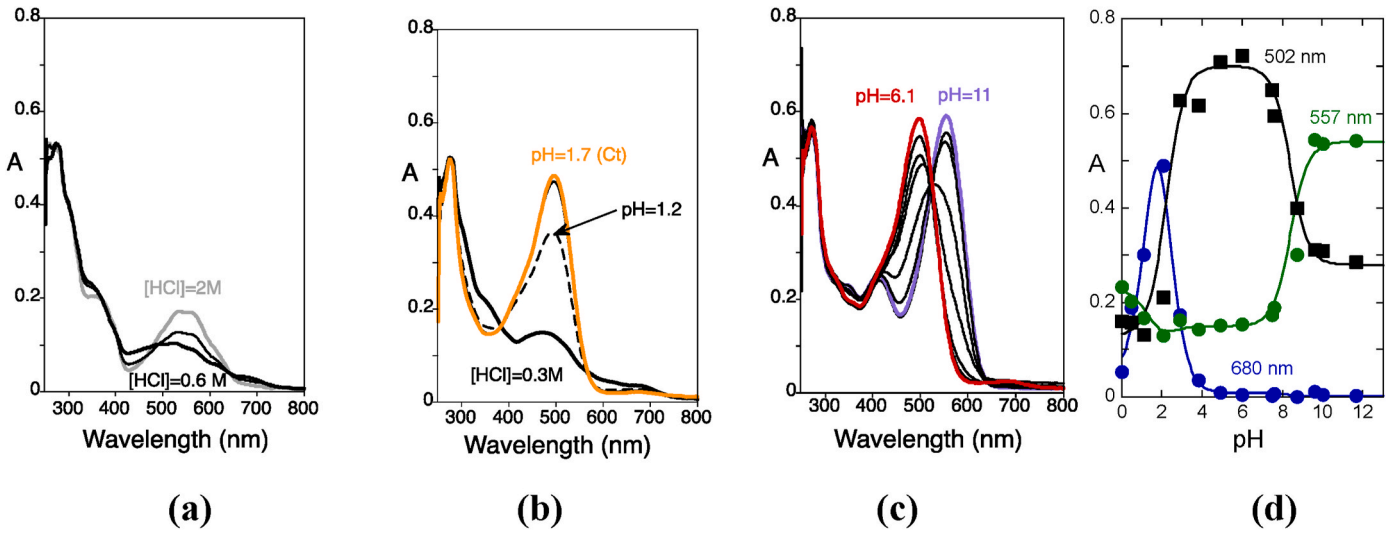

Fig. 14. **(a)** Spectral variations of BisNStB (4.2×10^{-5} M) in the presence of CTAB micelles (0.1 M) at extremely acid solutions; **(b)** The same for very acidic solutions; **(c)** Spectral variations between Ct and Ct^{-}; **(d)** titration curves at three representative wavelengths (502, 557 and 680 nm). Fitting was achieved for p*K* between Ct^{2+}/Ct^{+} ≈-0.1, $Ct^{+}/Ct \approx 1.0$ and $Ct/Ct^{-} = 8.6$.

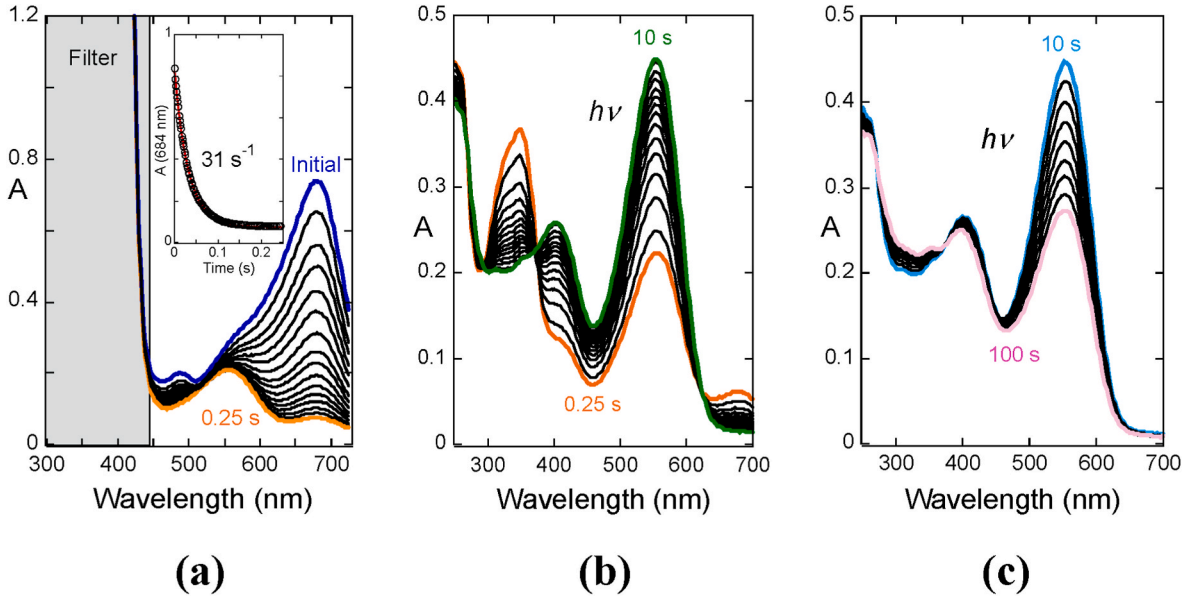

Fig. 15. **(a)** Spectral variations of BisNStB (4.2×10^{-5} M) upon a pH jump to pH = 13.7 monitored by stopped-flow with a filter 450 nm to cut the absorbance of the colorless species. Only one kinetics is observed during the first 100s (not shown); **(b)** In the absence of the filter the colorless species disappears to give the equilibrium species at this pH anionic *trans*-chalcone probably in equilibrium with the *cis*.; **(c)** further irradiation decreases the anionic *trans*-chalcone probably to reach another photostationary state involving an equilibrium between the anionic *cis*-chalcone in equilibrium with B2 and anionic *trans*-chalcone.

0.25 s in Fig. 15a is the same as the initial one of Fig. 10c. The fact that it is necessary 1 h to reach the equilibrium is again explained by the existence of B4, a kinetic reservoir that delays the kinetic process toward the equilibrium. The high intensity of the analyzing lamp gives some information regarding the photochemistry. The colorless species are converted in more anionic *trans*-chalcone Fig. 15b. This behavior could be attributed to photo-induced ring opening of B2 (already described for hemiketals) that not only forms more anionic *trans*-chalcone but also runs out B4. At this point the *trans*-chalcone disappears to give *cis*-chalcone that would convert rapidly in the dark to the anionic *trans*-chalcone the equilibrium species.

In Scheme 8 the extraordinary pH range of the *trans*-chalcones can be visualized. Except for very acid pH values, the *trans*-chalcones are the equilibrium species.

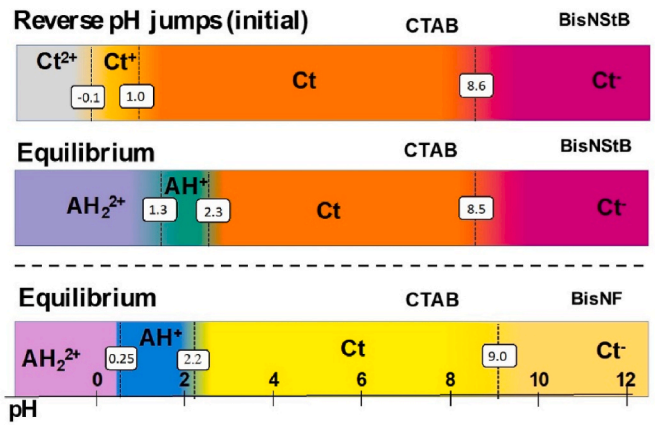

Scheme 8. pH domain of BisNStB in CTAB micelles at the equilibrium and its flavylium parent (BisNF), down, and the pH domain of the reverse pH jumps of the *trans*-chalcones immediately after the jump.

3. Photochemistry

The photochemistry of amino flavylium compounds in water is in general very inefficient [11]. In the case of BisNStB there is photodecomposition in the presence of SDS (pH = 10.2) or CTAB (pH = 4) micelles. In ethanol:water at pH = 6.2, styrylbenzopyrylium cation is formed upon irradiation of *trans*-chalcone at 436 nm, with quantum yield, $\Phi < 4 \times 10^{-5}$.

4. Conclusions

The introduction of a double bond between ring C and ring B gives rise to a system that can switch between violet (protonated styrylbenzopyrylium cation unstable) green (styrylbenzopyrylium cation) orange (*trans*-chalcone) and magenta (anionic *trans*-chalcone). It is possible to tune the pH domain of these colors by the addition of micelles, envisaging multiple applications of these types of compounds in the fields of chemistry and materials science.

The evidence for the B4 formation and the results recently observed for the anionic quinoidal base of malvidin 3,5-*O*-diglucoside, suggests that in basic medium the OH^- attacks not only in position 2 to give B2 but also in position 4 leading to B4. Stopped-flow has shown to be an indispensable tool to account for the fast kinetic processes in flavylium and styrylbenzopyrylium-based chemical systems.

5. Material and methods

5.1. Reagents and solutions

Sodium dodecyl sulfate (SDS) (≥98.5 %) and hexadecyltrimethylammonium bromide (CTAB) (≥98.5 %) were obtained from the commercial company Sigma-Aldrich. A universal buffer of Theorell and Stenhagen was prepared from the mixture of phosphoric acid 85 % (w/w), monohydrated citric acid, boric acid and NaOH solution 1 M, in 1 L of Millipore water with an ionic strength of 0.7 M.

5.2. Synthesis of 7-diethylamino-2-(4′-dimethylaminostyryl)-1-benzopyrylium (BisNStB)

The synthesis of BisNStB was performed as described in a previous work [16].

5.3. Direct and reverse pH jump

5.3.1. Ethanol:Water (1:1)

For direct pH jump experiments, firstly, it was prepared a stock solution (5.0×10^{-4} M) of BisNStB in ethanol, and then it was prepared a set of solutions at different pH values (adjusted by addition of HCl, NaOH or universal buffer of Theorell and Stenhagen), with 3.8×10^{-5} M of the pigment in 50 % ethanol. Each of these solutions was prepared in disposable cuvettes of 1 cm and the pigment was the last to be added. After preparing each cuvette, the direct pH jump was followed by Cary 60 UV-VIS (Agilent) spectrophotometer, and at the end, the pH values of these solutions were checked in a WTW pH 320 pH Meter handheld/Mettler Toledo InLab® Semi-Micro.

Regarding reverse pH jumps, the stock solution (5.0×10^{-4} M) of BisNStB was prepared in NaOH 0.1 M, with 95 % of ethanol and stabilized for approximately 20 h, until reaching the anionic *trans*-chalcone species. The set of solutions at different pH values was prepared in the same way as those in the direct pH jump experiment and read in the same way on the spectrophotometer.

All experiments were performed at room temperature and protected from light.

5.3.2. SDS and CTAB micelles

Two stock solutions were prepared: BisNStB (5.0×10^{-4} M) with SDS (0.1 M) and BisNStB (5.0×10^{-4} M) with CTAB (0.1 M), both dissolved in distilled water.

After this, several solutions at different pH values were prepared with 4.2×10^{-5} M of the pigment (BisNStB) and 0.1 M of SDS or 0.1 M of CTAB. The remaining procedure was the same as in the ethanol: water experiment.

For reverse pH jump experiments stock solutions of the pigment in the concentration of 5.0×10^{-4} M were prepared with 0.1 M of SDS or 0.1 M of CTAB, in NaOH 0.1 M (pH ≈ 13) and then a set of BisNStB solutions, with 4.2×10^{-5} M of pigment concentration, in the presence of each micelle (0.1 M) were prepared in the same way of direct pH jumps experiments.

The kinetics of reverse pH jump experiments were followed in the same way as the direct pH jumps, in the same spectrophotometer.

The experiments in SDS micelles were performed at room temperature, while in CTAB micelles were performed at 25 °C due to the ability of CTAB to crystallize at lower temperatures.

Both experiments were protected from light.

5.3.3. Stopped-flow experiments

The stopped-flow experiments were performed on a SX20 Applied Photophysics (Surrey, UK) spectrometer equipped with a PDA 1/UV photodiode array detector.

5.3.4. Photochemistry studies

Continuous irradiation experiments were conducted in a Spex Fluorolog-2 Model F111 spectrofluorometer equipped with a 150 W Xe lamp. The light flux (I_0) at λ_{irr} = 460 nm was determined using Aberchrome 540 dissolved in toluene as the actinometer [17]. Photochemical quantum yields (Φ) were determined from equation (6), where $\Delta A/\Delta t$ is the slope of the plot obtained by measuring the absorbance of the product at the irradiation time, V is the irradiated volume, ε is the molar extinction coefficient of the product and A_{irr} is the initial absorbance at the irradiation wavelength.

$$\varnothing = \frac{n\ moles\ of\ product\ per\ unit\ time}{n\ moles\ of\ absorbed\ photons\ per\ unit\ time} = \frac{\frac{\Delta A}{\Delta t \bullet \varepsilon} \bullet V}{I_0\left(1 - 10^{-A_{irr}}\right)} \quad (6)$$

5.3.5. Computational studies

DFT calculations have been carried out with the program Gaussian 16 using the B3LYP functional and the 6-31G** basis set. All calculations were performed considering the solvent effect with the PCM solvation method. The binary solvent mixture of ethanol:water (1:1) was defined by dielectric constant $\varepsilon = 54.89$ and the refractive index n = 1.3474 ($\varepsilon_\infty = n^2$) for 50 % Ethanol volume at 293 K [18]. Molecular structures were drawn using Chemcraft.

CRediT authorship contribution statement

Paula Araújo: Writing – review & editing, Writing – original draft, Methodology, Investigation, Formal analysis, Conceptualization. **Alexandra Borges:** Methodology, Investigation. **Joana Oliveira:** Writing – review & editing, Supervision, Investigation. **André Seco:** Methodology, Investigation. **Mani Outis:** Writing – original draft, Methodology, Investigation. **João C. Lima:** Writing – review & editing, Writing – original draft, Supervision, Methodology, Investigation. **Nuno Basílio:** Writing – review & editing, Validation. **Victor de Freitas:** Writing – review & editing, Supervision, Funding acquisition. **Fernando Pina:** Writing – review & editing, Writing – original draft, Validation, Supervision, Methodology, Investigation, Funding acquisition, Conceptualization.

Declaration of competing interest

The authors declare no conflict of interest.

Data availability

Data will be made available on request.

Acknowledgements

This work was supported by the Associate Laboratory for Green Chemistry - LAQV (LA/P/0008/2020 DOI 10.54499/LA/P/0008/2020; UIDP/50006/2020 DOI 10.54499/UIDP/50006/2020; UIDB/50006/2020 DOI 10.54499/UIDB/50006/2020) which is financed by national funds from FCT/MCTES. Authors thank FCT/MCTES for research contracts CEECIND/00466/2017 (N.B.), CEEC 2022.00042.CEECIND/CP1724/CT0017 (J.O.); Ph.D. fellowships: 2020.07313.BD (A.S.), SFRH/BD/143309/2019 (P.A.) and UI/BD/151270/2021 (A.B.).

Appendix A. Supplementary data

Supplementary data to this article can be found online at https://doi.org/10.1016/j.dyepig.2024.112280.

References

[1] Cruz L, Basilio N, Mateus N, de Freitas V, Pina F. Natural and synthetic flavylium-based Dyes: the chemistry behind the color. Chem. Rev. 2022;122:1416–81.
[2] Sousa D, Basilio N, Oliveira J, De Freitas V. A new insight on the degradation of anthocyanins: the reversible versus the irreversible chemical processes. J Agric Food Chem 2022;2022(70):656–68.
[3] Brouillard R, Dubois JE. Mechanism of structural transformations of anthocyanins in acidic media. J Am Chem Soc 1977;99:1359–64.
[4] Macanita AL, Moreira PF, Lima JC, Quina FH, Yihwa C, Vautier-Giongo C. Proton transfer in anthocyanins and related flavylium salts. Determination of ground-state rate constants with nanosecond laser flash photolysis. J Phys Chem A 2002;106:1248–55.
[5] Fernandes I, Faria A, Calhau C, de Freitas V, Mateus N. Bioavailability of anthocyanins and derivatives. J Funct Foods 2014;7:54–66.
[6] Correia P, Oliveira H, Araújo P, Brás NF, Pereira AR, Moreira J, de Freitas V, Mateus N, Oliveira J, Fernandes I. The role of anthocyanins, deoxyanthocyanins and pyranoanthocyanins on the modulation of tyrosinase activity: an in vitro and in silico approach. Int J Mol Sci 2021;22.
[7] Jurd L. Acid fruit and vegetable food and method of coloring emplying benzopyrylium compounds. Us Patent January, 31, 1967;3(301):683.
[8] Matsushima R, Fujimoto S, Tokumura K. Dual photochromic properties of 4-dialkylamino-2-hydroxychalcones. Bull Chem Soc Jpn 2001;74:827–32.
[9] Tokumura K, Taniguchi N, Kimura T, Matsushima R. Primary processes in photochromic reaction of 4-diethylamino-4 '-Dimethylamino-2-Hydroxychalcone in toluene. Chem Lett 2001;(126):126–7. https://doi.org/10.1246/cl.2001.126. 10.1246/cl.2001.
[10] Tron A, Gago S, McClenaghan ND, Parola AJ, Pina F. A blue 4 ',7-Diaminoflavylium cation showing an extended pH range stability. Phys Chem Chem Phys 2016;18:8920–5.
[11] Araújo P, Oliveira J, Basílio N, Parola AJ, de Freitas V, Pina F. Modulating the thermodynamics, kinetics and photochemistry of 7-diethylamino-4'-dimethylaminoflavylium in water/ethanol, sds and ctab micelles. Phys Chem Chem Phys 2020;24:17593–604.
[12] McClelland RA, Gedge S. Hydration of the flavylium ion. J Am Chem Soc 1980;102:5838–48.
[13] Alejo-Armijo A, Mendoza J, Parola AJ, Pina F. Chemical evolution of the colour systems generated by riccionidin a, 3-deoxyanthocyanidins and anthocyanins. Phytochem. 2020;174:11.
[14] Seco A, Pereira AR, Camuenho A, Oliveira J, Dias R, Bras NF, Basilio N, Parola AJ, Lima JC, Freitas V, Pina F. Comparing the chemistry of malvidin 3-O-glucoside and malvidin 3,5- O-diglucoside networks: a holistic approach to the acidic and basic paradigms with implications in biological studies. J Agric Food Chem 2024;72:7497–510.
[15] Gago S, Basilio N, Moro AJ, Pina F. Flavylium based dual photochromism: addressing "Cis-Trans" isomerization and ring opening-closure by different light inputs. Chem. Commun. 2015;51:7349–51.
[16] Araújo P, Rita Pereira A, de Freitas V, Mateus N, Fernandes I, Oliveira J Synthesis. Structural characterization and chromatic features of new 2-phenyl-1-benzopyrylium and 2-phenyl-styryl-1-benzopyrylium amino-based blue dyes. Tetrahedron Lett.s 2021;85:153487.
[17] Montalti M, C A, Prodi L, Gandolfi MT. Handbook of photochemistry, CRC press. Handbook of photochemistry. Crc Press; 2006. 2006.
[18] Navarkhele AV, Navarkhele VV. Static dielectric constants, densities, refractive indices and related properties of binary mixtures at various temperatures under atmospheric pressure. Int. J. Thermodyn 2022;25:1–10.